Geosynthetics, J. Kuwano & J. Koseki (eds)

Seismic stability analysis of base-reinforced embankments on soft soils

Biondi, G., Brighina, A. & Maugeri, M.
Department of Civil and Environmental Engineering, University of Catania, Italy

Keywords: reinforced embankments, base-reinforcement, seismic stability, soft soils, limit state design

ABSTRACT: In the paper the seismic stability conditions of embankments with geosynthetic basal reinforcement on soft soils are analyzed. A simplified design approach, based on a pseudo-static analysis of earthquake effects, is described using a limit state analysis. Several limit states are considered involving internal instability of the embankment and foundation soil instability. Expressions are derived for each failure mechanism giving the design values of the horizontal length of the embankment side-slope and of the maximum tensile load in the reinforcement. The inertial effect, including the influence of the vertical acceleration, and the effect of cyclic reduction of the foundation soil shear strength are considered in the analysis. By means of an extensive parametric analysis some design charts were developed and the influence of the model parameters is discussed.

1 INTRODUCTION

The analysis of the seismic behavior of road and railway embankments on poor cohesive ground represents an interesting, challenging geotechnical problem. The design of these structures under static conditions generally involves the prediction of the occurrence of large settlements and/or instability; under seismic conditions, the occurrence of permanent displacements and instability should be evaluated. Depending on the results of the design calculations, an improvement of the foundation soil could be necessary to ensure safety conditions and post-seismic serviceability.

With the exclusion of problems involving long-term consolidation settlements, the use of geosynthetics as a base-reinforcement represents an interesting alternative to more expensive soil improvement techniques. As regards the static behavior of base-reinforced embankments a number of studies were performed showing the main aspects of the failure mechanisms (Terzaghi et al., 1996, Leroueil & Rowe, 2001). Conversely, earthquake effects were insufficiently investigated. This is due to the difficulties in the seismic response analysis of these earth structures that should include the cyclic behavior of foundation soil, embankment fill and geosynthetic reinforcement and their dynamic interaction. In this framework, the cyclic degradation of the mechanical properties of the soil-geosynthetic interface and a reduction of the strength in the foundation soil should also be considered. In Europe, the British Standard Code of Practice BS 8006: 1995 represents the main guideline for the design of base-reinforced embankment on soft soils. However, the requirements and provisions of this code do not take into account earthquake effects.

For all these reasons the development of a simplified design approach, based on a pseudo-static analysis of earthquake effects, represents a useful tool to (i) describe the main aspects of the seismic behavior of base-reinforced embankments, (ii) select the appropriate strength characteristic of the geosynthetic reinforcement, (iii) provide a starting point for a more reliable dynamic response analysis. Based on these assumptions the paper describes a limit equilibrium pseudo-static analysis of base-reinforced embankments on poor cohesive ground. The solutions proposed in the paper are original and represent an extension to seismic conditions of those described in BS 8006:1995 for design calculations under static conditions.

2 DESCRIPTION OF THE DESIGN APPROACH

The way in which a base-reinforced embankment can fail during an earthquake depends on different parameters involving the stress-strain behavior of the foundation soil and of the embankment fill, the response of the reinforcement to the increase in

strength demand, the dynamic soil-reinforcement interface behavior and, finally, the characteristics of the seismic event. As far as the cohesive foundation soil is concerned, a strength reduction due to cyclic degradation and pore pressure build-up must be considered. As described by Matasovic & Vucetic (1995) both these effects can be accounted for using the degradation index t. Then the undrained soil shear strength C_u^d available during the cyclic loading condition imposed by the earthquake can be expressed as a function of its static value C_u^s and number of loading cycles N:

$$C_u^d / C_u^s = N^{-t} \quad (1)$$

N ranges from few to hundreds of cycles depending on the earthquake magnitude. For normally consolidated cohesive soils the degradation index t typically increases from 0 to about 0.4 for cyclic shear strain amplitude increasing from about 0.1% to about 3% (Ishihara, 1985; Matasovic & Vucetic, 1995). For N in the range 1-100 cycles, the ratio C_u^d / C_u^s (called degradation parameter) decreases from 1 to a minimum value which ranges from about 0.9 to about 0.25 depending on the value of t (Ishihara, 1985).

The influence of the cyclic behavior of the soil-geosynthetic interface can be accounted for through an accurate selection of the interface strength parameters; in this way the possible reduction from peak to residual strength values can be accounted for. With this aim results from cyclic friction tests or shaking table tests must be considered due to the discrepancy in the results of available studies concerning the strength values to be adopted in the stability analysis of earth-reinforced structures (Yegian & Kadakal, 1998; Zornberg, 2002).

The design principles of the limit state analysis will be adopted in the paper. The following considerations suggested the failure mechanisms to be considered. Field experience showed that it is the shearing resistance of the foundation soil that principally governs the stability of the embankment; moreover, geosynthetic basal reinforcement stabilizes the embankment by preventing lateral spreading of the fill, extrusion of the foundation soil and overall rotational failure; to ensure that the limit state tensile force can develop along the basal reinforcement, an adequate bond is required between the reinforcement and the adjacent soil. For these reasons, limit states involving internal instability of the embankment, foundation instability and instability in the embankment-foundation system are the most significant; therefore, the mechanisms to be considered are (Fig. 1): local instability of the embankment (*mechanism a*1), lateral sliding of the embankment (*mechanism a*2), extrusion of the soil foundation (*mechanism b*1), overall instability of the foundation soil (*mechanism b*2) and rotational instability of the embankment-foundation system (*mechanism c*).

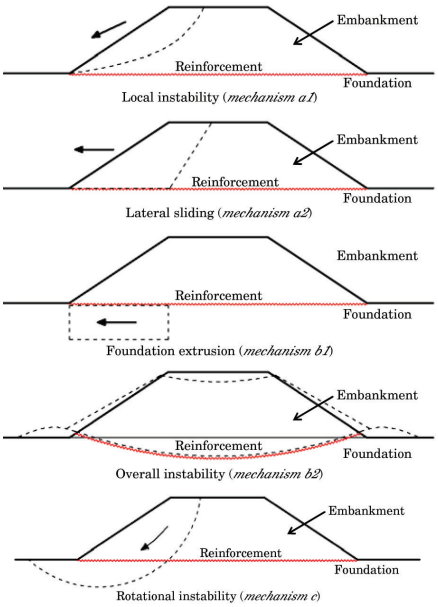

Figure 1. Limit states for base-reinforced embankments.

To generalize the solutions proposed in the paper, the following conditions were included in the analysis: horizontal (k_h) and vertical (k_v) seismic coefficients, live surcharge q at the top of the embankment, pore pressure in the embankment fill, foundation soil with undrained shear strength C_u increasing with depth z: $C_u(z) = C_{uo} + \rho \cdot z$.

3 ANALYSIS OF THE FAILURE MECHANISMS

Using the limit state design approach, the equations giving the minimum value L_s of the horizontal length of the embankment side-slope and the maximum value T of the required strength in the basal reinforcement were derived for seismic conditions considering the mechanisms $a1$, $a2$, $b1$ and $b2$. Solutions for static conditions are also presented and are compared with those described in BS 8006: 1995.

3.1 *Local instability of the embankment*

The local instability of the embankment (*mechanism a*1) could occur due to a rotational or translational failure mechanism; the latter mechanism will be considered. Denoting with ϕ'_{cv} the large strain angle of friction for the embankment fill under effective stress conditions, the limit state condition is described by the following equation:

$$\frac{H}{L_{s,a1}} = \frac{[1 - r_u/(1 - k_v)] \cdot \dfrac{\tan \phi'_{cv}}{f_{ms}} - \tan \theta}{1 + \dfrac{\tan \phi'_{cv}}{f_{ms}} \cdot \tan \theta} \qquad (2)$$

where H is the embankment height, r_u represents the static pore pressure ratio in the embankment fill, f_{ms} is the partial material factor applied to tan ϕ'_{cv} and θ is given by: tan $\theta = k_h/(1 - k_v)$.

Using eq. (2) the influence of the inertial effect on the values of the side-slope length $L_{s,a1}$ required for the stability of the embankment can be analyzed. Fig. 2, shows the plot of $L_{s,a1}$ versus H for the case $\phi'_{cv} = 38°$ and $r_u = 0$ and for different values of k_h and k_v. In particular the first five plots show the influence of k_h computed for a given value of the ratio k_v/k_h and point out the considerable influence of the inertial effect (quantified through k_h). The last plot, for the case $k_h = 0.4$, shows the influence of the ratio k_v/k_h on $L_{s,a1}$ highlighting the importance of the vertical component of ground motion in design calculations; as an example for the case $H = 4$ m and k_v/k_h ranging from –0.5 to +0.5, $L_{s,a1}$ varies from about 12 to about 20 m. For $k_h = k_v = 0$ eq. (2) gives the same static solutions described in BS 8006: 1995 (see the curves for $k_h = 0$ in Fig. 2).

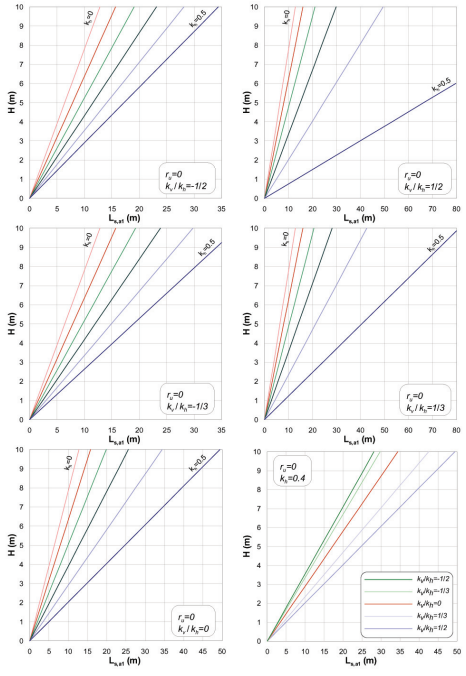

Figure 2. Influence of k_h and k_v on L_s for *mechanism a*1.

3.2 *Lateral sliding of the embankment*

The reference scheme for the limit state involving lateral sliding (*mechanism a*2) is shown in Fig. 3. To prevent lateral sliding due to the static stress state and to the earthquake-induced inertial effect, horizontal stresses within the embankment must be balanced by shear reaction on its base.

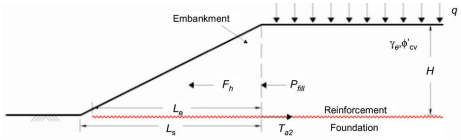

Figure 3. Limit state for lateral sliding of the embankment.

The design check for instability consists in the evaluation of the lateral thrust P_{fill} and checking the bond resistance on the embankment-soil interface. The expressions of the maximum tensile load T_{a2} needed to resist P_{fill} and of the maximum reinforcement bond length L_{a2} required to prevent horizontal sliding, can be obtained through an equilibrium equation for the limit state condition:

$$T_{a2} = \frac{H}{2}\left[(f_{fs}\gamma_e H + 2 f_q q)(1 - k_v)k_{ae} + \gamma_w \frac{H_w^2}{H}\right] \times \left(\frac{\dfrac{\alpha' \tan \phi'_{cv}}{f_{ms} f_s f_n}}{\dfrac{\alpha' \tan \phi'_{cv}}{f_{ms} f_s f_n} - \tan \theta}\right)$$

$$L_{e,a2} = \frac{[f_{fs}\gamma_e H + 2 f_q q](1 - k_v)k_{ae} + \gamma_w \dfrac{H_w^2}{H}}{\left[f_{fs}\gamma_e + \dfrac{\gamma_w H_w}{H}\left(\dfrac{2 - H_w}{H}\right)\right]\left[\dfrac{(1 - k_v)\alpha' \tan \phi'_{cv}}{f_{ms} f_s f_n} - k_h\right]} \qquad (3)$$

In eq. (3) k_{ae} is the active earth pressure coefficient for the seismic condition, γ_e is the embankment unit weight, H_w is the water table level with respect to the embankment base, α' is the interaction coefficient relating the embankment-reinforcement bond angle to tan ϕ'_{cv}, f_{fs}, f_q and f_s are the partial factors for γ_e, q and for the reinforcement sliding resistance respectively and finally, f_n is the partial factor for the economic ramifications of failure.

Figures 4 and 5 show the plots of $L_{s,a2}$ and T_{a2} versus H for the same cases as Fig. 2. For a given value of the ratio k_v/k_h the plots show less influence of H on L_s with respect to *mechanism a*1; also in this case the influence is more noticeable for the higher values of H. Concerning T_{a2}, Fig. 4 shows a significant influence of k_h for H greater than about 5 m and a considerable influence of k_v only for k_h greater than about 0.30.

The influence of the ratio k_v/k_h on $L_{s,a2}$ and T_{a2} is described in Fig. 5 for different values of H and for the cases $q = 0$, $r_u = 0$, $k_h = 0.2$ and $k_h = 0.4$. It is evident that for the lower values of k_h, the influence of k_v is modest on $L_{s,a2}$ and negligible on $T_{a2;}$ for higher values of k_h, both $L_{s,a2}$ and T_{a2} are significantly affected by k_v. As an example for $H = 4$ m, $k_h = 0.4$ and k_v/k_h ranging from –0.5 to +0.5, T_{a2} ranges from 330 to 730 kN/m about. Again the static solutions of the BS 8006: 1995 can be obtained assuming $k_h = k_v = 0$ in eqs. (3) (see the curves for $k_h = 0$ in Fig. 4).

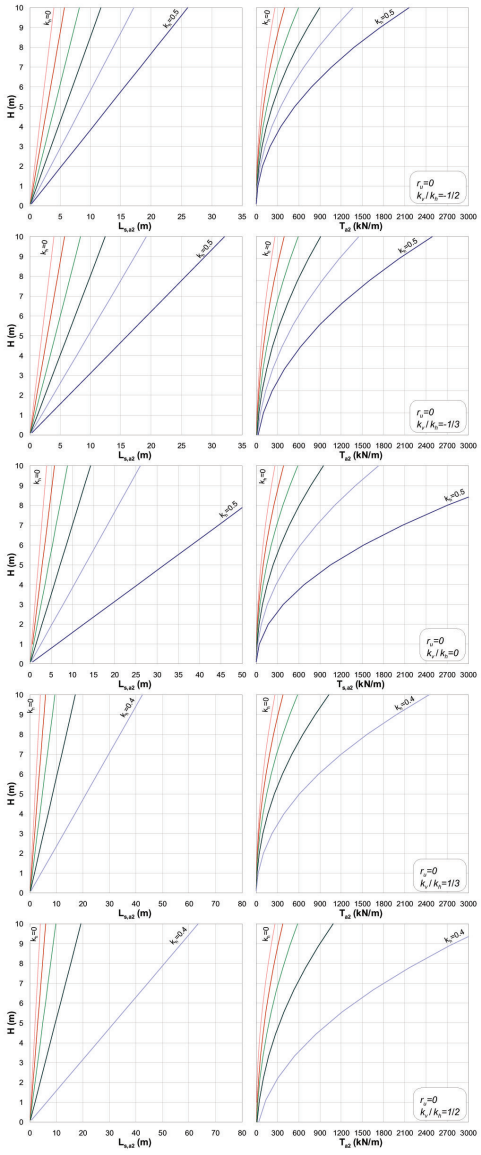

Figure 4. Influence of H, k_h, k_v on L_s and T for *mechanism a*2.

3.3 *Extrusion of the soil foundation*

Due to the shear stress transmitted by the embankment and to the inertial effect arising in the foundation soil, lateral extrusion of the foundation may occur. In this case the considered failure mechanism (Fig. 6) assumes lateral extrusion of the soil beneath the embankment and within a depth z_c.

To prevent this limit state from occurring, the overall shearing resistance on the underside of the reinforcement should be sufficient to resist the lateral

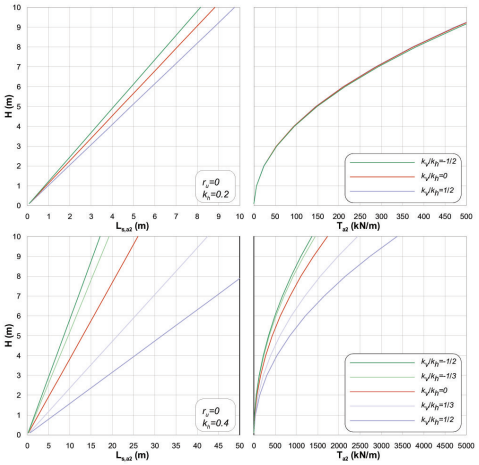

Figure 5. Influence of k_v/k_h on L_s and T for *mechanism a*2.

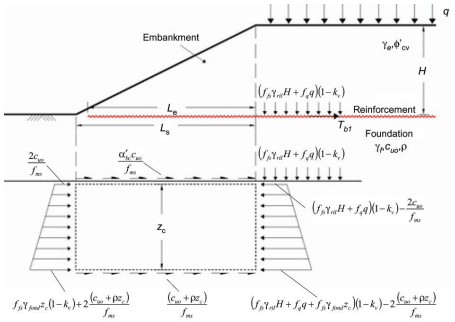

Figure 6. Lateral extrusion of the foundation (*mechanism b*1).

loads developed in the foundation soil; moreover, the geosynthetic reinforcement should have sufficient tensile strength to withstand the tensile load induced by the shear stress transmitted by the foundation soil. Therefore, the side-slope length of the embankment has to be greater than the minimum value $L_{s,b1}$ necessary to prevent the mobilization of these outward shear stresses; referring to Fig. 6 the obtained expression of $L_{s,b1}$ is:

$$L_{s,b1} = \frac{(f_{fs}\gamma_e H + f_q q)(1-k_v) - \dfrac{4C_{uo} + 2\rho z_c}{f_{ms}}}{\dfrac{C_{uo}(1+\alpha'_{bc})}{f_{ms}} + \left(\dfrac{\rho}{f_{ms}} - f_{fs}\gamma_f k_h\right) z_c} z_c \tag{4}$$

where α'_{bc} is the interaction coefficient relating the soil-reinforcement adherence to C_{uo}, γ_f is the soil foundation unit weight and f_{ms} is the partial factor applied to $C_u(z)$. Since z_c could be unknown, the evaluation of $L_{s,b1}$ through eq. (4) generally requires an iterative procedure; in this case the maximum values of $L_{s,b1}$ should be checked according to the condition:

$\partial L_{s,b1}/\partial z_c = 0$. On the other hand the tensile load generated in the reinforcement due to the outward foundation shear stress is:

$$T_{b1} = \frac{\alpha'_{bc} \cdot C_{uo}}{f_{ms}} \cdot L_s \qquad (5)$$

Due to the dynamic behavior of the interface between the geosynthetic and the cohesive foundation soil interface, a reduction in adherence may occur; moreover, cyclic degradation of the shear strength of the foundation soil may occur depending on the soil loading history imposed by the earthquake. In the proposed approach both these aspects can be accounted for through an appropriate selection of the interaction coefficient α'_{bc} and through an accurate evaluation of the shear strength profile (i.e. values of C_{uo} and ρ). The influence of α'_{bc}, C_{uo} and ρ, on z_c, $L_{s,b1}$ and T_{b1} is described in Fig. 7 for the case q = 0 kPa, γ_e = 17 kN/m^3, γ_f = 20 kN/m^3 and α'_{bc} equal to 1, $^3/_4$, $^1/_2$, $^1/_3$ and $^1/_4$. The plots shows that a reduction in the soil-geosynthetic adherence does not significantly affect z_c and $L_{s,b1}$ especially for the lower values of H; generally, a reduction of α'_{bc} produces a reduction in the depth z_c and a modest increase in the required side-slope length $L_{s,b1}$. However, the influence of α'_{bc} on T_{b1} is considerable and a significant increment of the required tensile strength is observed for decreasing values of α'_{bc}. As an example, for the case H = 4 m, C_{uo} = 5 kPa, ρ = 1 kN/m^3 an increase of T_{b1} of about 50% is obtained for α'_{bc} ranging from 1 to 0.5; for the same condition and H = 6 m an increase of about 90% in T_{b1} is evaluated.

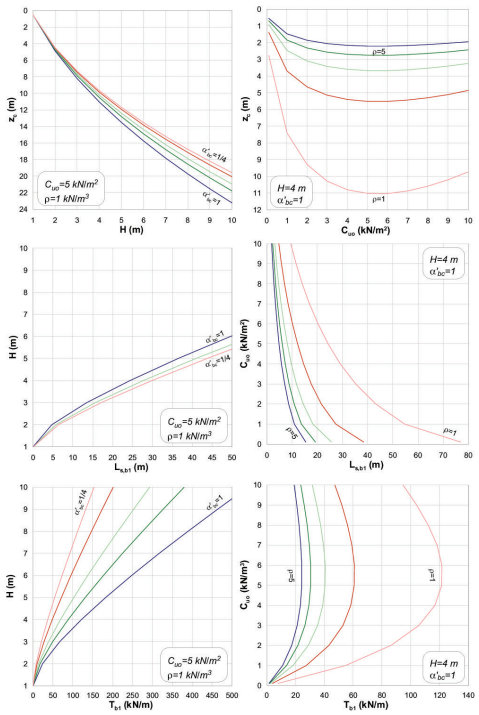

Figure 7. Influence of α'_{bc}, C_{uo} and ρ, on z_c, $L_{s,b1}$ and T_{b1}.

In the proposed approach the strength reduction in the foundation soil is evaluated using eq. 1 and is quantified through an appropriate selection of the parameters C_{uo} and ρ. The effect of this strength degradation on z_c, $L_{s,b1}$ and T_{b1} is described in Fig. 7 for the case H = 4 m and α'_{bc} = 1; the change in the slope of the plots of z_c and T_{b1} versus C_{uo} is related to the limitation of the analytical solution imposed by the denominator of eq. 4 which must be always positive. The plots of Fig. 7 clearly show the significant dependence of z_c, $L_{s,b1}$ and T_{b1} on the adopted values of C_{uo} and ρ. As an example for the case ρ = 2 kN/m^3 a reduction of C_{uo} from 5 to 2.5 kPa produces an increase of the required side-slope length $L_{s,b1}$ from about 13.5 m to about 22.5 m and a reduction of z_c of about 0.5 m; for the case ρ = 1 kN/m^3 the same reduction of C_{uo} produces an increase in the tensile strength T_{b1} from about 50 kN/m to about 70 kN/m.

3.4 *Overall instability of the foundation soil*

The occurrence of an overall instability may be checked to ensure deep-seated rotational failures cannot occur. To analyze this limit state a comparison with the case of a load transmitted by a shallow footing to the foundation soil can be performed; then a bearing capacity solution including an increasing strength with depth should be derived. Using the limit equilibrium approach and referring to the scheme of Fig. 8 the embankment was considered as an equivalent footing of width $B = b + L_s$ (being b the crest width of the embankment) and the limit value q_{b2} of the vertical load transmitted to the foundation was derived imposing a rotational equilibrium condition:

$$q_{b2} = \frac{(2+\pi) \cdot C_{uo} + B \cdot \rho}{f_{ms}} \qquad (6)$$

Assuming that the weight of the embankment cannot exceed q_{b2}, the following minimum value of the side-slope length of the embankment can be derived:

$$L_{s,b2} = \frac{(f_{fs}\gamma_e H + f_q q)(1-k_v) - (2+\pi)\, C_{uo}/f_{ms}}{2\rho/f_{ms}} \qquad (7)$$

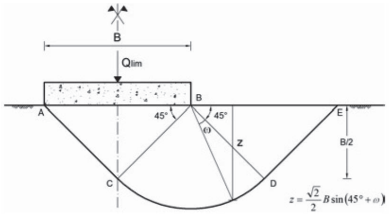

Figure 8. Failure mechanism considered in the overall instability of the foundation soil.

Using eq. 7 a minimum value of H, below which no physical solution exists, can be detected. The influence of k_h and k_v on $L_{s,b2}$ is described in Fig. 9 for the case q = 0 kpa, b = 20 m, C_{uo} = 5 kPa and ρ = 1 kN/m^3. The changes in the slope of the plots are related to the minimum values of H previously described. For values of H that satisfy eq. 7, Fig. 9 points out the influence of the inertial effect on the minimum side-slope length $L_{s,b2}$ required for the overall instability of the embankment; at the same time the importance of the vertical component of seismic acceleration is again highlighted.

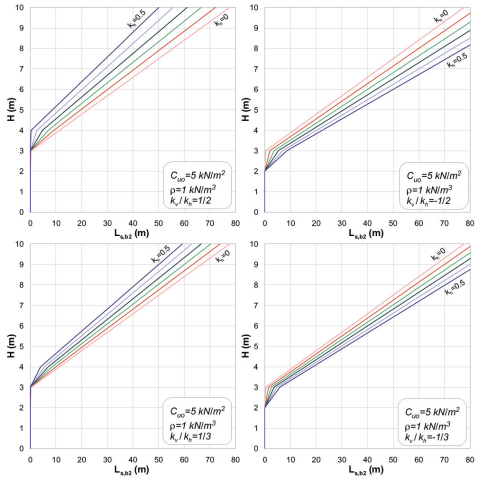

Figure 9. Influence of k_h and k_v on $L_{s,b2}$.

4 CONCLUDING REMARKS

The paper describes the seismic stability conditions of base-reinforced embankments on poor ground using the pseudo-static approach and the limit state design. Five different failure mechanisms were considered and original solutions were derived in order to estimate the design values of the horizontal side-slope length of the embankment and of the reinforcement tensile load. In the analysis horizontal and vertical seismic coefficients were considered together with a surcharge at the top of the embankment, pore pressure in the embankment fill and a foundation soil with undrained strength increasing with depth; moreover, a practical approach, to take into account the reduction in the soil-geosynthetic adherence and in the foundation soil shear strength, was described.

For each mechanism a parametric analysis was performed and the obtained results were discussed. As regards the side-slope length of the embankment a significant influence of the horizontal seismic acceleration was observed for the limit state related to the local instability of the embankment and to the overall instability of the foundation soil; otherwise a less evident influence was observed in the other limit states especially for the lower values of the embankment height. The vertical component of the seismic acceleration significantly affects the design values of the side-slope length of the embankment in the limit states related to the local instability of the embankment and overall instability of the foundation soil; similar results were obtained for the lateral sliding failure mechanism at higher levels of horizontal seismic acceleration. As far as the tensile load in the geosynthetic reinforcement is concerned, the results obtained show that the horizontal acceleration significantly affects this parameter in the limit state related to the lateral sliding of the embankment; moreover, the influence of the vertical component is negligible for the lower values of the horizontal component while it is considerable for the higher values. Finally strength reductions in the soil-geosynthetic interface or in the foundation soil produce a significant increment in both the value of the side-slope length of the embankment and in the values of the maximum reinforcement load.

REFERENCES

British Standard BS 8006: 1995. "Code of practice of Strengthened/reinforced soils and other fills", 162 pp.

Leroueil, S. and Rowe, R.K. (2001). "Embankments over soft soil and peat", Chapter 16 in Geotechnical and Geoenvironmental Handbook, R.K., Rowe Editor, Kluwer Academic Publisher, pp. 463-499.

Ishihara, K. (1985). "Soil Behaviour in Earthquake Geotechnics". Oxford Science Publications, 242 pp.

Matasovic, N. and Vucetic, M. (1995). "Generalized cyclic-degradation-pore pressure generation model for clays", *J. of Geotechnical Engineering, ASCE,* 121, No.1, pp. 33-42.

Terzaghi, K., Peck, R.B. and Mesri, G. (1996). "Soil mechanics in engineering practice", 3rd Ed, Wiley, 549 pp.

Yegian, M.K. and Kadakal, U. (1998). "Geosynthetic Interface Behavior Under Dynamic Loads". Geosynthetic International, Vol 5, Nos 1-2, pp. 1-16.

Zornberg, J.G. (2002). "Peak versus residual shear strength in geosynthetic-reinforced soil design". Geosynthetic International, Vol. 2, No. 4, pp. 301-318.